Journal of Systems Engineering and Electronics
Vol. 34, No. 5, October 2023, pp.1235 – 1251

UCAV situation assessment method based on C-LSHADE-Means and SAE-LVQ

XIE Lei[1], TANG Shangqin[1], WEI Zhenglei[2,*], XUAN Yongbo[3], and WANG Xiaofei[3]

1. Institute of Aeronautics Engineering, Air Force Engineering University, Xi'an 710038, China; 2. China Aerodynamics Research & Development Center, Mianyang 621000, China; 3. Blue Sky Innovation Center for Frontier Science, Beijing 100000, China

Abstract: The unmanned combat aerial vehicle (UCAV) is a research hot issue in the world, and the situation assessment is an important part of it. To overcome shortcomings of the existing situation assessment methods, such as low accuracy and strong dependence on prior knowledge, a data-driven situation assessment method is proposed. The clustering and classification are combined, the former is used to mine situational knowledge, and the latter is used to realize rapid assessment. Angle evaluation factor and distance evaluation factor are proposed to transform multi-dimensional air combat information into two-dimensional features. A convolution success-history based adaptive differential evolution with linear population size reduction-means (C-LSHADE-Means) algorithm is proposed. The convolutional pooling layer is used to compress the size of data and preserve the distribution characteristics. The LSHADE algorithm is used to initialize the center of the mean clustering, which overcomes the defect of initialization sensitivity. Comparing experiment with the seven clustering algorithms is done on the UCI data set, through four clustering indexes, and it proves that the method proposed in this paper has better clustering performance. A situation assessment model based on stacked autoencoder and learning vector quantization (SAE-LVQ) network is constructed, and it uses SAE to reconstruct air combat data features, and uses the self-competition layer of the LVQ to achieve efficient classification. Compared with the five kinds of assessments models, the SAE-LVQ model has the highest accuracy. Finally, three kinds of confrontation processes from air combat maneuvering instrumentation (ACMI) are selected, and the model in this paper is used for situation assessment. The assessment results are in line with the actual situation.

Keywords: unmanned combat aerial vehicle (UCAV), situation assessment, clustering, K-means, stacked autoencoder, learning vector quantization.

DOI: 10.23919/JSEE.2023.000062

Manuscript received February 24, 2021.
*Corresponding author.
This work was supported by the Natural Science Foundation of Shaanxi Province (2020JQ-481;2021JM-224), and the Aeronautical Science Foundation of China (201951096002).

1. Introduction

With the continuous development of artificial intelligence technology, the intelligence and autonomy of unmanned combat aerial vehicle (UCAV) represented by the US "loyal wingman" have been significantly improved, but the existing intelligence is far from being able to meet actual needs [1], therefore, autonomous air combat technology is a research hot issue currently studied by countries around the world [2]. UCAV air combat situation assessment is an important part of autonomous air combat. It is based on a comprehensive situational information perception to analyze the situation of the enemy and ourself, and provide reliable guidance information for UCAV maneuver decision-making [3]. It has high requirements for assessment accuracy and timeliness. The existing situation assessment methods are mainly divided into two categories: non-parametric method and parametric method. At present, scholars from all over the world have conducted in-depth research on these two methods.

The non-parametric method uses the situation function to quantify the angle, speed, altitude, distance [4] and weapon performance. Zhao et al. proposed an air combat situation assessment method based on decision tree, and assessed the situation from multiple aspects [5]. Zhang et al. established angle situation and distance situation based on relative position information, which assist maneuver decision [6]. Zhang et al. constructed an advantage evaluation function based on the key factors of the air combat situation, and used the cross-entropy method to distribute the weight of each factor, building a dynamic threat air combat situation assessment model [7]. From the above research, the situation assessment performance of the non-parametric method is mainly determined by the situation function. Although the method is simple to implement, has good timeliness, and has strong scalability, the weight definition of the situation function is too subjective,

ignoring the continuity of the information. In complex cases, it is difficult to accurately describe situation information.

The parametric method is based on the prior knowledge of air combat, it uses uncertainty theory to approximate the relationship between air combat information, and constructs a situation assessment model. Ying et al. used improved belief entropy (IBE) to process data, and used classic dempster combination rules to fuse data [8]. However, this method is difficult to apply in complex situations. Xu et al. took the single aircraft confrontation as an example, it proposed a novel semi-supervised naive Bayes classifier, which takes less time to evaluate, but has low accuracy [9]. Lu et al. proposed a target threat assessment technology based on cloud model and Bayesian theory [10], which uses cloud model to realize the expression and processing of situation, and Bayesian modifies the membership cloud. He et al. proposed a naive Bayesian situation model based on historical situation, and analyzed and modeled the tactical theory to make the situation assessment targeted [11]. Xuan et al. established a grey fuzzy Bayesian network model for air combat situation assessment [12]. The uncertain knowledge of grey fuzzy theory is introduced into the uncertain reasoning of Bayesian network. Sun et al. infered the purpose of enemy fighter pilots by constructing Bayesian networks [13]. Narayana et al. used Bayesian formula, which is combined with maximum posterior probability and relevant situation judgment rules to infer the current situation [14]. Ma et al. proposed a target threat assessment technology based on the cloud model and Bayesian theory [15]. It uses the cloud model to realize the expression and processing of the situation, and Bayesian theory modifies the membership degree of the cloud model. The assessment method has high requirement of the cloud models. Based on the above research, it can be known that the parametric situation assessment method has good evaluation ability in the uncertainty problem method, and has low complexity and simple calculation process, but there are also many problems such as incomplete prior knowledge, difficult to apply in the complex air combat, and high dependence on model initialization.

To solve the problem that it is difficult to maintain high timeliness, objectivity and accuracy in the current air combat situation assessment, we have made the following original contributions in the paper:

(i) The off-axis angle of the missile is combined with the angle factor, and the launch distance constraint of the missile is combined with the distance factor, the evaluation factors containing weapon factors are established, and it converts multi-dimensional input data into characteristic information of air combat situation.

(ii) It proposes the convolution success-history based adaptive differential evolution with linear population size reduction-means (C-LSHADE-Means) clustering method to extract knowledge of air combat situation. The UCI data set verifies that this method has good clustering performance.

(iii) It proposes an stacked autoencoder and learning vector quantization (SAE-LVQ) situation assessment model to achieve the supervised situation assessment rapidly. Compared with multiple assessment methods, the results show that this method has the highest accuracy and shorter time.

(iv) In the air combat maneuvering instrument (ACMI) system, three kinds of air combat confrontation data are selected, and this model is used to assess the situation of UCAV and enemy aircraft, comprehensively consider the global situation. The assessment results are analyzed, and it is line with the actual situation.

The rest of this paper is organized as follows: Section 2 introduces the overall design. Section 3 analyzes air combat confrontation and constructs angle and distance evaluation factors. Section 4 proposes the C-LSHADE-Means to extract the knowledge of air combat situation. Section 5 proposes a situation assessment model based on SAE-LVQ. Section 6 conducts situation assessment under multiple working conditions. Finally, Section 7 gives the conclusions of this paper and future research directions.

2. Overall design

To overcome the shortcomings of the existing situation assessment methods, a data-driven situation assessment method is established. The UCAV dynamic model is used to generate a large amount of confrontation data, and the angle and distance evaluation factors are established which can accurately reflect situation information. Based on the above premise, the clustering method is used to extract the knowledge of the air combat situation. Then, an accurate classifier is built. Finally, multiple sets of confrontation data are selected from the ACMI system to analyze the situation with the model proposed in this paper. The flowchart is shown in Fig. 1, and the specific steps are as follows:

Step 1 Build a UCAV dynamic model, air combat is analyzed to extract 12-dimensional information, the angle evaluation factor $f_a(X)$ and the distance evaluation factor $f_d(X)$ are established.

Step 2 A C-LSHADE-Means clustering method is proposed, which uses angle evaluation factors and distance evaluation factors to convert 12-dimensional air combat information into two-dimensional features, it extracts air combat situation knowledge through clustering, and labels the data.

Step 3 The labeled 12-dimensional data is used as

the input of the SAE-LVQ classifier, training set and test set are constructed to verify the accuracy and time consumption of the classifier.

Step 4 Air combat data in different working conditions are selected from the ACMI system, and the SAE-LVQ is used to assess the situation from the UCAV and enemy aircraft to verify the effectiveness of the model proposed in this paper.

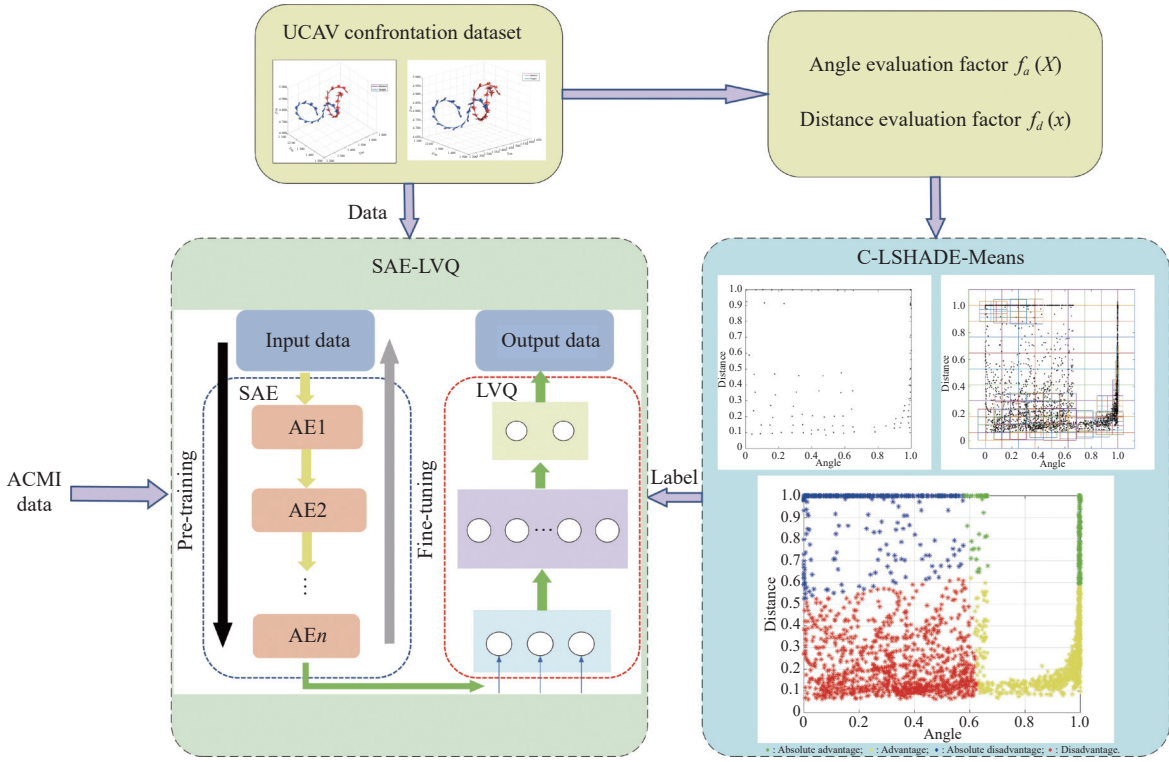

Fig. 1 Overall design flow chart

3. UCAV air combat situation evaluation factor

3.1 Air combat analysis

In one-to-one air combat, situation assessment is a comprehensive judgment based on the relative information of the enemy and ourselves. The information of the enemy and ourselves is shown in Fig. 2.

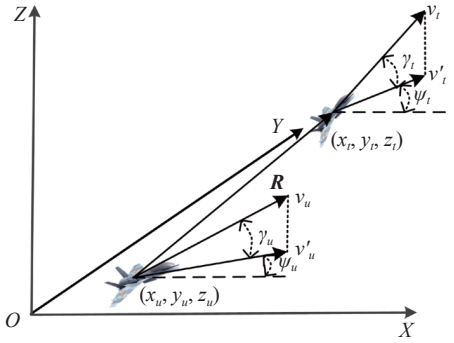

Fig. 2 Three-dimensional two-aircraft confrontation model

(x_u, y_u, z_u) represents space coordinate position of UCAV, v_u represents speed of UCAV, γ_u and ψ_u represent UCAV's pitch angle and yaw angle. (x_t, y_t, z_t) represents the space coordinate position of the enemy aircraft, v_t represents the speed of the enemy aircraft, γ_t and ψ_t represent the pitch and yaw angle of the enemy aircraft, and $\boldsymbol{R} = (x_t - x_u, y_t - y_u, z_t - z_u)$ represents the distance between the two aircraft. A 12-dimensional air combat information parameter matrix is

$$\boldsymbol{X} = [x_u, y_u, z_u, v_u, \gamma_u, \psi_u, x_t, y_t, z_t, v_t, \gamma_t, \psi_t]. \tag{1}$$

To solve the problem of confrontational data sources, a dynamic model of UCAV is constructed. The specific formula is as follows:

$$\begin{cases} \dot{x} = V\cos\gamma\cos\psi \\ \dot{y} = V\cos\gamma\sin\psi \\ \dot{z} = V\sin\gamma \\ \dot{v} = \dfrac{T\cos\alpha - D}{m} - g\sin\gamma \\ \dot{\gamma} = \dfrac{(L + T\sin\alpha)\cos\mu}{mv} - \dfrac{g}{v}\cos\gamma \\ \dot{\psi} = \dfrac{(L + T\sin\alpha)\sin\mu}{mv\cos\gamma} \end{cases} \tag{2}$$

where α is the angle of attack, m is the aircraft mass, T is

the engine thrust, D is the air resistance, and L is the lift. (x,y,z) represents the spatial coordinate position of UCAV; v represents the speed; γ, ψ, μ represent pitch angle, yaw angle, and roll angle; g represents gravitational acceleration. In this model, (x,y,z,v,γ,ψ) is the state quantity and (δ,α,μ) is the control quantity [16].

During the flight, due to fuel consumption, its own weight will be reduced, which is determined by the consumption coefficient c. The formula is as follows:

$$\dot{m} = -cT. \tag{3}$$

Thrust, drag and lift are affected by aircraft shape, flight status and environmental factors. The calculation formula is as follows:

$$T = \delta T_{\max}(\bar{v}, h_c), \tag{4}$$

$$L = \frac{1}{2}\rho v^2 S C_L, \tag{5}$$

$$D = \frac{1}{2}\rho v^2 S C_D. \tag{6}$$

In the above formula, δ is the throttle position, ρ is the air density, S is the aerodynamic cross-sectional area of the UCAV, C_L and C_D are the coefficients of lift and drag, and $T_{\max}$ is the maximum thrust of the UCAV.

In this paper, the new UCAV-"Storm Shadow" is a combat aircraft, and its aerodynamic parameters and engine thrust characteristics are obtained for simulation experiments.

3.2 Angle evaluation factor

In the three-dimensional coordinate system, the main factors affecting the angle evaluation are the entry angle and the direction angle, which can be projected into the two-dimensional coordinate system for simplification. Therefore, the two-aircraft confrontation model shown in Fig. 3 is established.

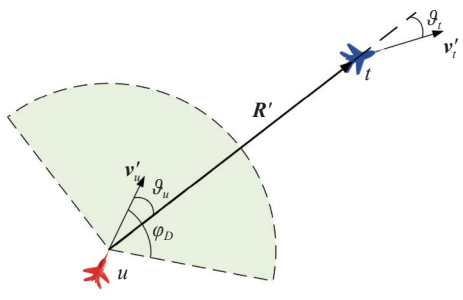

Fig. 3 Two-aircraft confrontation model in two-dimensional aircraft

$\boldsymbol{R}' = [x_t - x_u, y_t - y_u]$ is the horizontal distance between UCAV and the target; ϑ_u is the target azimuth, which is the angle between the UCAV horizontal velocity $\boldsymbol{v}_u = (v_{ux}, v_{uy})$ and the target line of sight; ϑ_t is target lead angle[17], which is the angle between the enemy's horizontal velocity $\boldsymbol{v}_t = (v_{tx}, v_{ty})$ and the line-of-sight extension; the sector area is the missile attack zone, and φ_D is the maximum off-axis launch angle.

The calculation formula of ϑ_u is

$$\vartheta_u = \begin{cases} \arccos \dfrac{\boldsymbol{R}' \cdot \boldsymbol{v}_u}{\|\boldsymbol{R}'\| \cdot \|\boldsymbol{v}_u\|}, & v_{uy} \cdot (x_t - x_u) - v_{ux} \cdot (y_t - y_u) \leqslant 0 \\ -\arccos \dfrac{\boldsymbol{R}' \cdot \boldsymbol{v}_u}{\|\boldsymbol{R}'\| \cdot \|\boldsymbol{v}_u\|}, & v_{uy} \cdot (x_t - x_u) - v_{ux} \cdot (y_t - y_u) > 0 \end{cases}. \tag{7}$$

Since UCAV is flying in all directions, ϑ_u is positive counterclockwise, and it ranges from $-\pi$ to π. When $v_{uy} \cdot (x_t - x_u) - v_{ux} \cdot (y_t - y_u) \leqslant 0$, it indicates that $\boldsymbol{v}_u$ is in the counterclockwise direction of $\boldsymbol{R}'$ and ϑ_u belongs to $[-\pi, 0]$, and ϑ_u can be directly calculated according to the vector angle formula. When $v_{uy} \cdot (x_t - x_u) - v_{ux} \cdot (y_t - y_u) > 0$, it indicates that $\boldsymbol{v}_u$ is in the clockwise direction of $\boldsymbol{R}'$ and ϑ_u belongs to $[0, \pi]$. The calculation principle of ϑ_t is the same as that of ϑ_u. The calculation formula of ϑ_t is

$$\vartheta_t = \begin{cases} \arccos \dfrac{\boldsymbol{R}' \cdot \boldsymbol{v}_t}{\|\boldsymbol{R}'\| \cdot \|\boldsymbol{v}_t\|}, & v_{ty} \cdot (x_t - x_u) - v_{tx} \cdot (y_t - y_u) \leqslant 0 \\ -\arccos \dfrac{\boldsymbol{R}' \cdot \boldsymbol{v}_t}{\|\boldsymbol{R}'\| \cdot \|\boldsymbol{v}_t\|}, & v_{ty} \cdot (x_t - x_u) - v_{tx} \cdot (y_t - y_u) > 0 \end{cases}. \tag{8}$$

Considering the influence of the missile attack zone on the angle, a new angle evaluation factor η_A is constructed:

$$\eta_A = \begin{cases} \left(1 - \dfrac{|\vartheta_u|}{k_a \phi_{D_0}}\right)^{(1-k)} \cdot \left(1 - \dfrac{|\vartheta_t|}{\pi}\right)^k, & |\vartheta_u| \in [0, \varphi_D] \\ \left(1 - \dfrac{|\vartheta_u|}{\pi}\right)^{1-k} \cdot \left(1 - \dfrac{|\vartheta_t|}{\pi}\right)^k, & |\vartheta_u| \notin [0, \varphi_D] \end{cases}. \tag{9}$$

k_a is the gain coefficient in the attack zone, $k_a > \pi/\varphi_{D_0}$. The missile has a stronger attack ability against targets with a small off-axis angle. When the off-axis angle of the target is close to the maximum off-axis angle of the missile, the target is easy to get rid of the missile attack by escape maneuver. Therefore, k_a is needed to give full play to the missile's attack characteristics. k is the distance adjustment coefficient, indicating the urgency of adjusting the angle, the calculation formula is

$$k = \mathrm{e}^{-\frac{d - d_{\min}}{d_{\min}}} \tag{10}$$

where $d_{\min}$ is the minimum missile attack range.

In (9), two cases are divided according to the value of ϑ_u. When $|\vartheta_u| \in [0, \varphi_D]$, it means that the enemy is within the range of the UCAV missile attack zone, $\left(1 - \dfrac{|\vartheta_u|}{k_a \varphi_{D_0}}\right)$ represents the ability of UCAV tail chase. When $\vartheta_u = 0$,

it indicates that the UCAV is chasing after the tail, and the quantization value is the largest. $\left(1-\frac{|\vartheta_t|}{\pi}\right)$ represents the ability of enemy to escape. When $\vartheta_t=0$, it represents that the enemy is escaping in the front, and the quantization value is the largest. When $|\vartheta_u| \notin [0,\varphi_D]$, it means that enemy is out of the UCAV missile attack zone, and the principle is the same as the above.

The angle evaluation factor is simulated in Matlab. Assuming that $\varphi_{D_0}=\pi/3$, $k_a=2\pi/\varphi_{D_0}$, $d=4\,000$ m, $d_{\min}=1\,000$ m, $\vartheta_t \in [-\pi,\pi]$, $\vartheta_u \in [-\pi,\pi]$, the simulation result is shown in Fig. 4. When $\vartheta_t=0$, $\vartheta_u=0$, it means that the UCAV is tail chasing the enemy, the angle is the best and $\eta_A=1$; when $\vartheta_t=-\pi$, $\vartheta_u=\pi$, it means that UCAV is tail chased by the enemy, the angle is the worst and $\eta_A=0$, it is in line with the actual situation.

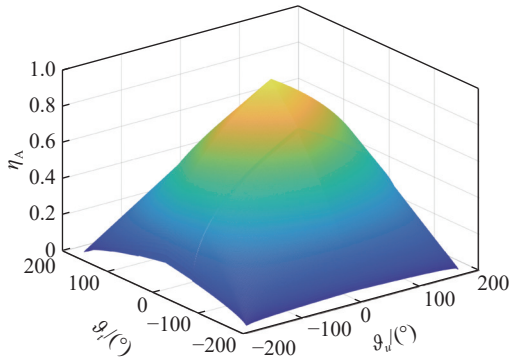

Fig. 4 Angle evaluation factor

3.3 Distance evaluation factors

In the process of air combat, distance is a very critical factor. Therefore, the distance evaluation factor is constructed by the missile attack distance, to guide UCAV to maintain a good attack distance.

$$\eta_R=\begin{cases} e^{3\frac{R-R_{\min}}{R_{\min}}}, & R<R_{\min} \\ 1, & R_{\min}\leqslant R\leqslant R_{\max} \\ e^{3\frac{R_{\max}-R}{R_{\max}}}, & R>R_{\max} \end{cases} \tag{11}$$

where R represents the relative distance between UCAV and the enemy, $R_{\min}$ and $R_{\max}$ represent the maximum and minimum launch distance of the missile. Formula (11) can indicate the relative distance is good or bad.

4. Air combat situation knowledge extraction based on C-LSHADE-Mean

According to the literature, clustering methods can be divided into partition methods, hierarchical methods, overlapping methods and graph-based methods [18−22]. In this paper, the partition method is used to cluster. The K-means is the most widely used. It completes the clustering by using the euclidean distance between data to measure the similarity, but it takes too much time to process a large amount of data and is very sensitive to the selection of the initial cluster center. In response to the above problems, this paper proposes a C-LSHADE-Means clustering method to extract knowledge of air combat situation.

4.1 Convolutional pooling layer to compress data

Convolutional neural networks (CNN) can quickly process a large amount of data. The most critical technologies are convolutional layer and pooling layer. The 12-dimensional air combat data has been transformed into two-dimensional data after being processed by angle factors and distance factors. Therefore, the convolutional pooling layer is used to compress data while maintaining the data distribution characteristics. The specific steps are as follows:

Step 1 Refer to the STING clustering method, the input sample space area is divided into rectangular units, each unit obtains the number of samples, and a quantity matrix is established, as shown in Fig. 5.

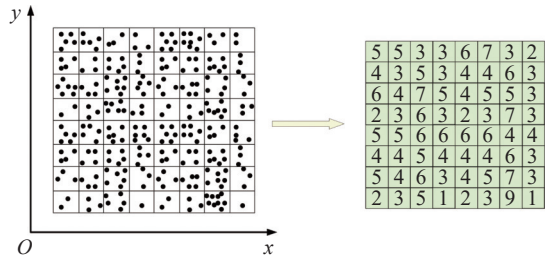

Fig. 5 Unit extraction quantity matrix

Step 2 After the quantity matrix is established, the mean convolution kernel is used, and in order to avoid repeated data entry, the traditional sliding window convolution is not used, and the equal interval convolution is used, as shown in Fig. 6.

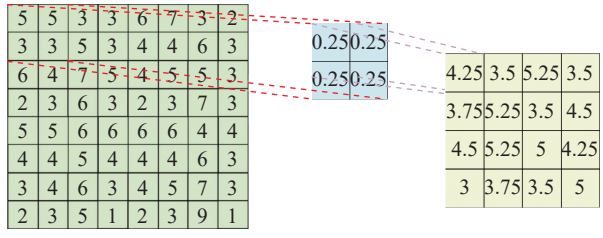

Fig. 6 Equal interval mean convolution

Step 3 After the convolutional layer compresses the data, average pooling is used to ensure that the distribution characteristics of different regions have not changed, as shown in Fig. 7.

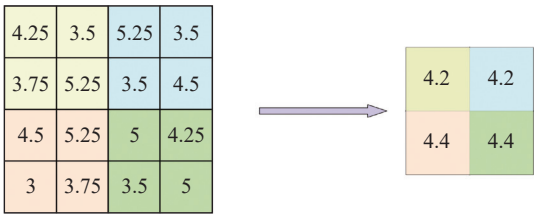

Fig. 7 Average pooling

Step 4 The density of each unit is calculated, multiply it by the compressed coefficientε, and round to get the number of compressed samples for each unit. The specific calculation formula is as follows:

$$\rho_{ij}=\text{round}\left(\frac{n_{ij}}{\sum_{i=1,j=1}^{i=m,j=l} n_{ij}}\cdot\varepsilon\right),$$
$$i=1,2,\cdots,m;\ j=1,2,\cdots,l \tag{12}$$

where n_{ij} represents the value of each unit of the quantity matrix after convolution and pooling.

Step 5 After obtaining the compressed number of unit samples, the reverse distribution is performed according to the density value of each layer, finally, when it is returning from the quantity matrix to the sample distribution, divide the units equally according to the value, and solve the mean value of sample coordinates in each unit. The specific process is shown in Fig. 8.

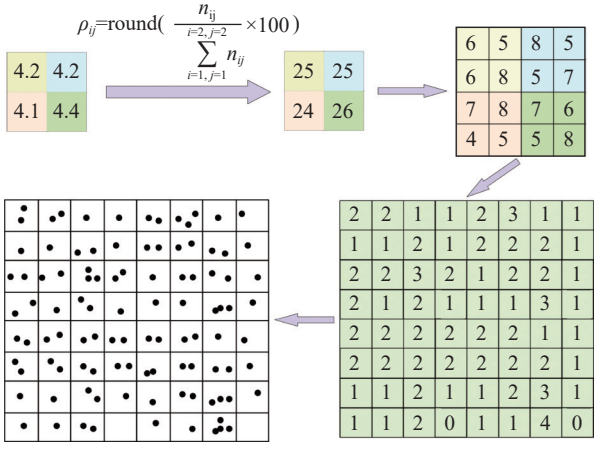

Fig. 8 Reverse distribution of compressed quantity matrix

4.2 LSHADE-Mean clustering method

4.2.1 K-means algorithm

The K-means algorithm is a traditional partition clustering method. It completes the classification by using the Euclidean distance between data points to measure similarity.

The K-means algorithm first randomly selects K samples as the initial cluster centers, calculates the distance between each sample and the cluster centers. According to the principle of minimum distance, the samples are classified into different cluster centers, and the cluster centers are adjusted to the mean value of all samples in this category. The calculation is repeated again until the cluster centers remain unchanged.

4.2.2 LSHADE algorithm

Success-history based adaptive differential evolution with linear population size reduction (LSHADE) algorithm is an efficient and improved version based on the differential evolution (DE) [23] algorithm. It uses mutation, crossover and greedy strategies to find the global optimal value, with faster optimization speed and better stability [24]. The LSHADE algorithm is a linear population size reduction strategy to increase the algorithm's timeliness performance. The specific steps are as follows:

Step 1 Initialize the population.

$$x_{ij}=l_j+\text{rand}\cdot(u_j-l_j) \tag{13}$$

where x_{ij} represents the jth dimension of the ith population, u_j and l_j represent the upper and lower search limits.

Step 2 Set scale factor F and cross rate Cr, the specific formula is

$$\text{Cr}=\text{randn}(\text{Mcr},0.1), \tag{14}$$

$$F=\text{randc}(\text{MF},0.1). \tag{15}$$

Among them, Cr obeys a normal distribution with a mean of Mcr and a variance of 0.1, F obeys a Cauchy distribution with a mean of MF and a variance of 0.1. MF and Mcr represent the mean values of the F and Cr which are randomly selected from the memory storage mechanism, and the initial settings of MF and Mcr are both 0.5, which will be updated later according to (14) and (15).

Step 3 Perform mutation operation. On the basis of current-to-pbest/1 [25] mutation strategy, a new mutation strategy is proposed:

$$\boldsymbol{v}_i=\boldsymbol{x}_i^G+F_i^G(\boldsymbol{x}_{\text{pbest}}^G-\boldsymbol{x}_i^G)+F_i^G(\boldsymbol{x}_{r1}^G-\boldsymbol{x}_{r2}^G) \tag{16}$$

where $\boldsymbol{x}_i^G$ represents the ith target vector in the Gth generation; F_i^G represents the ith scale factor of the Gth generation; $\boldsymbol{x}_{p\text{best}}^G$ represents a random selection of the top $p\%$ of the optimal vectors, where p is the control parameter for exploration and survey; r_1 represents randomly selected individuals in the current population, r_2 represents randomly selected individuals in an external storage mechanism, and the external storage mechanism

contains vectors that performed well in the previous iterations.

Step 4 Cross update. Crossover according to the crossover rate and the mutation vector:

$$\boldsymbol{u}_{i,j}^{G}=\begin{cases}\boldsymbol{v}_{i,j}^{G}, & \text{rand}_{i,j}\leqslant \text{Cr}_i \text{ or } j=j_{\text{rand}}\\ \boldsymbol{x}_{i,j}^{G}, & \text{otherwise}\end{cases} \tag{17}$$

where Cr_i represents the probability of crossover.

Step 5 Greedy strategy is used to update the population. The update formula is

$$\boldsymbol{x}_{i}^{G+1}=\begin{cases}\boldsymbol{u}_{i}^{G}, & f(\boldsymbol{u}_{i}^{G})\leqslant f(\boldsymbol{x}_{i}^{G})\\ \boldsymbol{x}_{i}^{G}, & \text{otherwise}\end{cases} \tag{18}$$

where $\boldsymbol{x}_{i}^{G+1}$ is the updated population, $f(\boldsymbol{u}_{i}^{G})$ and $f(\boldsymbol{x}_{i}^{G})$ represent the fitness value of variation vector and the Gth generation population.

Step 6 The linear population size reducing（LPSR） strategy is used to update the population size. LPSR formula is

$$N^{G+1}=\text{round}\left[\left(\frac{N^{\min}-N^{\text{init}}}{\text{nfes\_max}}\right)\cdot\text{nfes}+N^{\text{init}}\right] \tag{19}$$

where N^{G+1} represents the number of next-generation populations; nfes represents the current evaluation times; nfes_max is the maximum evaluation times; N^{init} is the initial population size; $N^{\min}$ is the minimum population number.

Step 7 Judge whether the termination condition is met, if the maximum number of evaluation times is reached or the loss target value is met, the optimization is stopped and the optimal solution is output, otherwise return to Step 2.

4.2.3 Combination of LSAHDE and K-means

Swarm intelligent clustering algorithm is a hot research direction of current clustering algorithm. It mainly uses swarm heuristic optimization algorithm to solve clustering problems [26]. To combine the LSHADE algorithm with the K-means clustering method, the sum-of-squares within cluster (SSW) [27] index is introduced as the fitness function of the optimization algorithm. The specific calculation formula is

$$\text{SSW}=\sum_{k=1}^{K}\sum_{i=1}^{m}\text{dist}(x_{k,i},c_k) \tag{20}$$

where c_k is the center of the kth cluster of the data, $x_{k,i}$ is the ith point in the kth cluster, and dist is the distance between the two points.

When the LSHADE initializes the population, the coding technology based on label [20] is used to introduce the cluster center of each cluster. The cluster center solution is transformed into an optimization problem, as shown in Fig. 9.

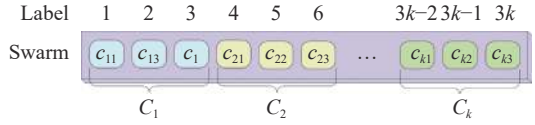

Fig. 9 Coding technology based on label

To verify that the LSHADE algorithm can better optimize K-means centers, the UCAV dynamic model is used to generate multiple sets of confrontation data, and a variety of swarm intelligent clustering algorithms related to K-means are selected for comparison. There are covariance matrix learning and the Bimodal distribution parameter different evaluation (CoBiDE) algorithm [28], DE algorithm [29], sparrow search algorithm (SSA) [30], particle swarm optimization (PSO) algorithm [31], harris hawks optimization (HHO) algorithm [32], grey wolf optimization (GWO) algorithm [33], and gravity search algorithm (GSA) [34]. The specific parameter settings are shown in Table 1.

Table 1 Algorithm parameter settings

Algorithm	Parameter setting
LSHADE	H=3, MF=0.5, p_{init}=0.11, N_{init}=200, $N_{\min}$=150, D=2
CoBiDE	pb=0.4, ps=0.5, D=2
DE	F=0.5, Cr=0.5, D=2
SSA	Leader position update probability=0.5
PSO	C_1=1.5, C_2=1.5, D=2, Inertia factor=0.3
HHO	α=0.01, β=1.5, J=2(1-rand)
GWO	a=2−2t/$t_{\max}$
GSA	α=20, G0=100, R_{norm}=2, R_{power}=1

It can be seen from Fig. 10 that the LSHADE algorithm has the fastest decline speed and the final SSW is the smallest, indicating that the method proposed in this paper can find a better clustering center in the air combat situation data.

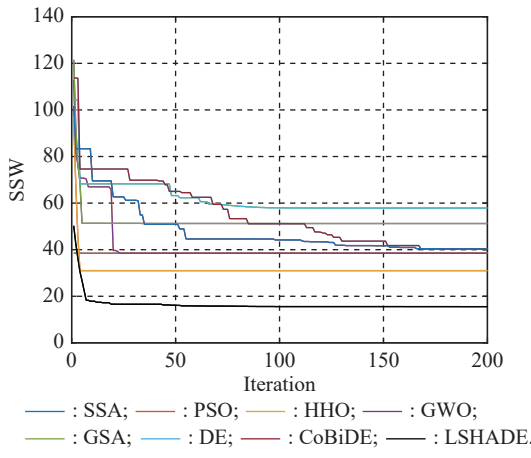

Fig. 10 SSW curve

4.3 Performance verification

To verify that the C-LSHADE-Means method has better clustering performance, a UCI data set is selected. Since the air combat situation data is two-dimensional data after being processed by angle factors and distance factors, therefore, the selected data set is also two-dimensional data. The UCI data set is sym data.

In order to evaluate the clustering performance of each algorithm, Accuracy (Ac), Silhouette (Sil), Davies-Bouldin (DB) [35], Calinski-Harabaz (CH) indexes are introduced. The specific information of each index is shown in Table 2.

Table 2 Cluster evaluation index

Index	Formula	Description
Ac	$A=\dfrac{N_r}{N}\times 100$	N_r is the number of correct sample classifications; N is the total number of samples; the larger the Ac, the better the clustering effect.
Sil	$\mathrm{SI}=\dfrac{1}{N}\sum_{i=1}^{N}\dfrac{b_i-a_i}{\max(b_i,a_i)}, a_i=\dfrac{1}{N_k}\sum_{x_j\in c_k}\mathrm{dist}(x_i,x_j)$ $b_i=\min_{h\in\{1,\cdots,k\},h\neq k}(\dfrac{1}{N_k}\sum_{x_j\in c_k}\mathrm{dist}(x_i,x_j))$	a represents the average distance from the sample to other samples of the same category, b represents the shortest average distance from the sample to other samples of different categories, $\mathrm{SI}\in[-1,1]$, the larger the SI, the better the clustering effect.
DB	$\mathrm{DB}=\dfrac{1}{k}\sum_{j=1}^{k}\max\dfrac{s(c_k)+s(c_r)}{\mathrm{dist}(c_k,c_l)}$ $s(c_k)=\dfrac{1}{n}\sum_{i=1}^{n}d(x_i,c_k)$	DB represents the proportion of cluster scatter between cluster separation.
CH	$\mathrm{CH}(k)=\dfrac{\mathrm{BGSS}}{\mathrm{WGSS}}\times\dfrac{n-k}{k-1}$ $\mathrm{WGSS}=\dfrac{1}{2}\sum_{i=1}^{k}(n_i-1)\bar{d}_i^2$ $\mathrm{BGSS}=\dfrac{1}{2}[(k-1)\bar{d}^2+\sum_{i=1}^{k}(n_i-1)(\bar{d}^2-\bar{d}_i^2)]$	$\bar{d}_i^2$ represents the average distance of samples in the ith cluster, $\bar{d}^2$ represents the average distance of all samples, and the larger the CH, the better the clustering effect.

Seven contrast clustering algorithms are chosen, which are density peak clustering (DPC)[36], fuzzy C-means (FCM) clustering, Gaussian mixture model (GMM) clustering, clustering by communication with local agent (CLA)[37], local gravitation clustering (LGC)[37], K-means clustering, and K-means algorithm based on the bargaining game (GBK-Means)[38]. The experimental simulation environment is Windows 10, CPU is 2.80 GHz, 16G memory, and the running environment is Matlab2019b. The clustering algorithm parameters are shown in Table 3.

Fig. 11 shows the clustering results of different clustering algorithms on the test data set. Each color in Fig. 11 corresponds to a cluster. The same category of different algorithms may have different color representations, but this does not affect the final result. It can be seen from the figure that the algorithm in this paper has a good clustering effect.

Table 3 Clustering algorithm parameter settings

Number	Algorithm	Parameter setting
1	DPC	Reference [36]
2	FCM	The index of the membership matrix is 2, the maximum number of iterations is 200, and the minimum membership is 1.0e−5
3	GMM	The non-negative regularization number is 1.0e−5
4	CLA	Reference [37]
5	LGC	Reference [37]
6	K-means	Use Euclidean distance, the number of clusters is 4
7	GBK-Means	Reference [38]
8	C-LSHADE-Means	Use Euclidean distance, the number of clusters is 4, the maximum number of iterations is 200, CR=0.5, F=0.5, the initial population is 200, and the minimum population is 150

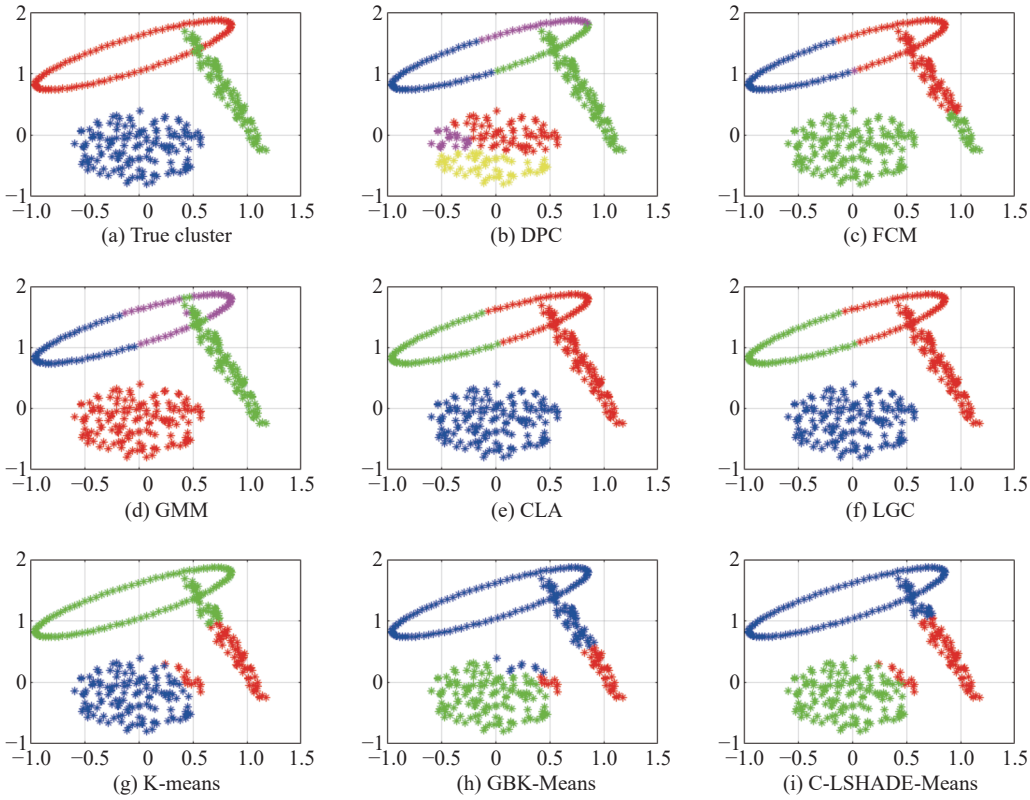

Fig. 11 Clustering results of UCI data

From Ac in Table 4, it can be seen that the proposed method has good clustering accuracy on the Sym data set. Its CH index is the best, indicating that the clustering results of the algorithm in this paper are dense within clusters and discrete between clusters. The Sil index is the best, indicating that the data in the cluster has a high degree of matching. DB indicators also perform well, indicating that the number of clusters is appropriate. Therefore, it can be seen that the clustering effect of the algorithm in this paper is better through the results of four indexes.

Table 4 Clustering results

Data	Index	DPC	FCM	GMM	CLA	GLA	K-means	CBK-Means	C-LSHADE-Means
UCI Data	Ac/%	63.24	74.57	80.35	84.1	84.2	75.43	77.43	86.86
	DB	0.6584	0.7850	0.7701	0.635	0.635	0.7627	0.750	0.7526
	CH	237.3047	339.5852	283.9508	336.248	336.249	340.2413	286.260	340.2610
	Sil	0.2468	0.4160	0.4084	0.402	0.410	0.4192	0.383	0.4348
	Rank	8/8	3/8	5/8	6/8	4/8	2/8	7/8	1/8

4.4 UCAV air combat situation knowledge extraction

According to the UCAV dynamic model, multi-condition confrontation data is generated, and the angle factor and distance factor are used to calculate the situation to form a situation data set.

The convolutional layer and the pooling layer are used to compress the data to reduce the calculation amount of cluster center optimization, and the LSHADE-Means algorithm is used for clustering, where K=4 [13], and the specific process is shown in Fig. 12.

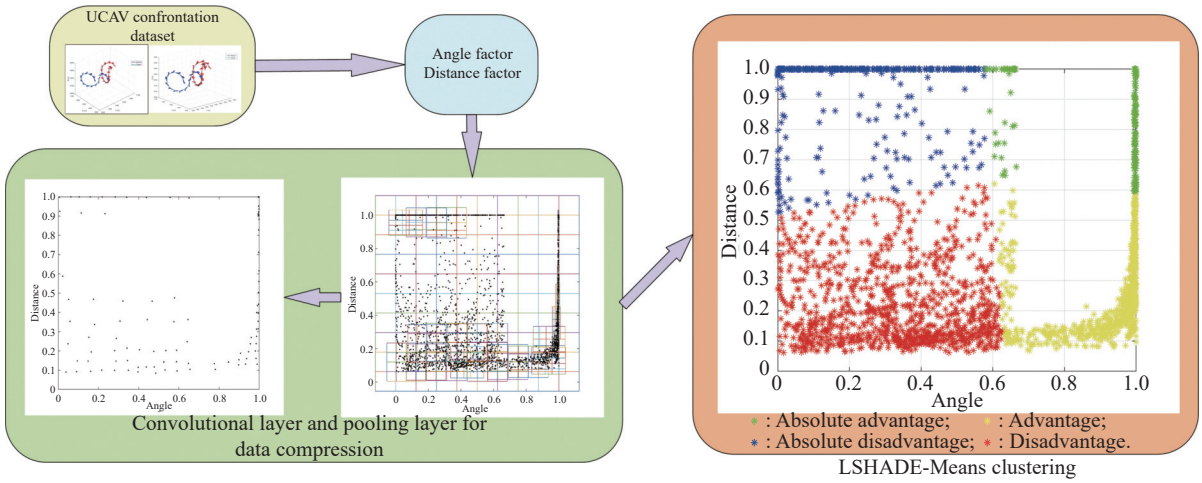

Fig. 12 Flow chart of situation extraction

5. Situation assessment model based on SAE-LVQ

The air combat information parameter has 12 dimensions, and there is a certain internal coupling relationship between each dimension, which is not conducive to extracting the air combat situation directly [39]. In the situation assessment process, the accuracy and timeliness are very important. In this section, the stacked autoencoder is used to reduce the dimensionality of data and ensure the saliency of the features. At the same time, the learning vector quantization network is used to achieve high-precision classification. The SAE-LVQ model is established.

5.1 Stack autoencoder

Compared with autoencoders, stacked autoencoders deepen the network structure and enhance the data representation ability, and the sparseness limitation realizes the function of feature extraction [40], hence, it is widely used in classification and data dimensionality reduction [41]. The structure of SAE is shown in Fig. 13.

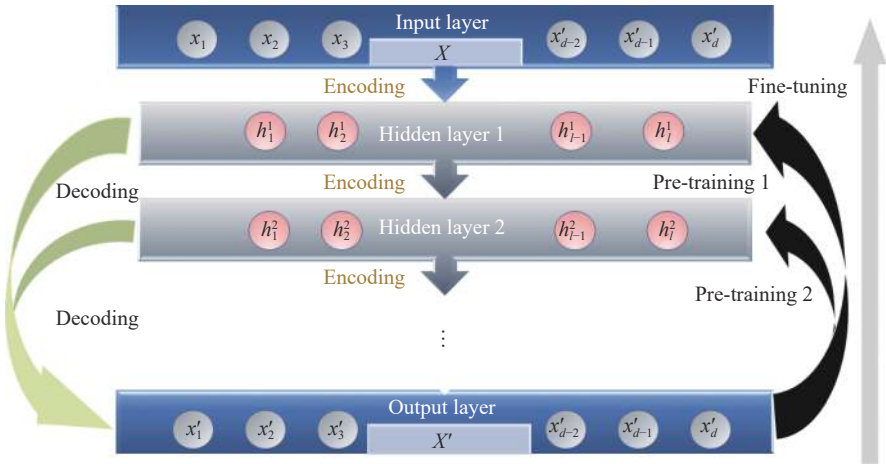

Fig. 13 SAE structure

In the case of multiple hidden layers, to achieve a better weight training effect, the greedy layer-wise training method is adopted. The training method is mainly divided into two parts: pre-training and fine-tuning.

Pre-training means to optimize network parameters layer by layer. The training process is shown in Fig. 13. First, the weight between the input layer and the first hidden layer is $H_{1,l}=[h_1^1,h_2^1,\cdots,h_{l-1}^1,h_l^1]$, l is the number of hidden layer nodes. The input data X is output after being encoded and decoded, and errors occur between input and output, the gradient descent method is used for training. The $H_{1,l}$ keeps unchanged when training the weight of the second hidden layer. After $H_{2,l}=[h_1^2,h_2^2,\cdots,h_{l-1}^2,h_l^2]$ encoding, the output is decoded, and error occurs again. Use the gradient descent method to train $H_{2,l}$. And so on, until all hidden layer weights are trained, the network pre-training ends.

After the network pre-training is completed, the error between the output data X' and the input data X is calculated, and the back propagation algorithm is used to fine-

tune the weights of each layer again.

5.2 LVQ network

The LVQ network is a variant structure of the self-organizing map network. The competitive layer is trained under supervision. It has the advantages of simple structure, fewer training steps and high classification accuracy. In image compression [42], sensor diagnosis system [43] and fault diagnosis of power transformer [44] have shown strong classification and recognition capabilities.

The LVQ network structure is divided into three layers: input layer, competition layer and output layer, as shown in Fig. 14.

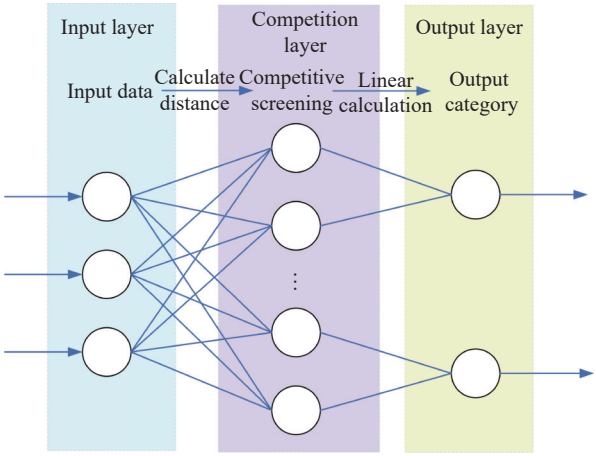

Fig. 14 LVQ network structure

The algorithms can be divided into LVQ1, LVQ2 and LVQ3, of which the LVQ2 network has a wide range of applications. Due to the consideration of "second winning" neurons, it has stronger recognition capabilities [45]. The specific calculation steps are as follows:

Step 1 Initialize the weight $\boldsymbol{W}^1_{S_1\times R}$ between the input layer and the competition layer and the learning rate η, where S_1 is the number of neurons in the competition layer and R is the input vector dimensions.

Step 2 Calculate the distance between the input vector $\boldsymbol{X}_{R\times 1}$ and the neurons in the competition layer. The formula is

$$d_i = \left\|\mathrm{dist}(\boldsymbol{X}_{R\times 1}, \boldsymbol{W}^1_{S_1\times R})\right\| = \sqrt{\sum_{i=1}^{R}(x_i - w^1_{ij})},$$
$$i = 1,2,\cdots,R; j = 1,2,\cdots,S_1 \tag{21}$$

where w^1_{ij} is the weight between the ith neuron in the input layer and the jth neuron in the competition layer.

Step 3 Select two neurons n, m with the smallest distance from the input vector.

Step 4 If n and m satisfiy the following conditions at the same time: the output of the neuron n and neuron m are the different categories; d_n and d_m satisfy $\min\left\{\frac{d_n}{d_m}, \frac{d_m}{d_n}\right\} > \rho$, where ρ is the width of the middle part of the two vectors, generally, it is 2/3.

When the output category of neuron n is correct, the weight correction formula is

$$\begin{cases} w_n^{\mathrm{new}} = w_n^{\mathrm{old}} + \eta(x - w_n^{\mathrm{old}}) \\ w_m^{\mathrm{new}} = w_m^{\mathrm{old}} - \eta(x - w_m^{\mathrm{old}}) \end{cases}. \tag{22}$$

When the output category of neuron m is correct, the weight correction formula is

$$\begin{cases} w_n^{\mathrm{new}} = w_n^{\mathrm{old}} - \eta(x - w_n^{\mathrm{old}}) \\ w_m^{\mathrm{new}} = w_m^{\mathrm{old}} + \eta(x - w_m^{\mathrm{old}}) \end{cases}. \tag{23}$$

Step 5 When the condition in Step 4 is not met, only update the weight of the minimum distance neuron. When the minimum distance neuron is classified correctly, the weight update formula is

$$w^{\mathrm{new}} = w^{\mathrm{old}} + \eta(x - w^{\mathrm{old}}). \tag{24}$$

When the classification is wrong, the weight update formula is

$$w^{\mathrm{new}} = w^{\mathrm{old}} - \eta(x - w^{\mathrm{old}}). \tag{25}$$

5.3 SAE-LVQ situation assessment model

Combining the stacked autoencoder and the LVQ network, an SAE-LVQ situation assessment model is proposed. The stack autoencoder technology is used to extract the characteristics of the air combat information, reduce the data dimension. The LVQ network is trained by the labeled data to achieve supervised classification. The SAE-LVQ situation assessment model is shown in Fig. 15.

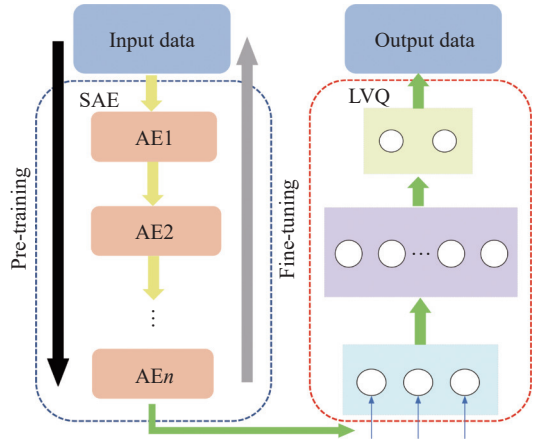

Fig. 15 SAE-LVQ situation assessment model

The specific steps are as follows:

Step 1 Initialize SAE-LVQ network parameters. Initialize the SAE hidden layer weight H, the LVQ weight $\boldsymbol{W}^1_{S_1\times R}$, and the learning rate η.

Step 2 Input air combat information to train the SAE, and output the reconstructed features.

Step 3 Input the labeled reconstruction features into the LVQ network, use the LVQ2 algorithm for supervised training, and output the situation category.

5.4 Situation assessment performance test

To verify the accuracy and timeliness of the SAE-LVQ situation assessment model, five classifiers are selected for comparison, including hierarchical support vector machine (HSVM) [46], crow search algorithm optimized support vector machine (CSA-SVM) [47], K-nearest neighbor (KNN) [48], stacked autoencoder-hierarchical support vector machine (SAE-HSVM), and LVQ network. The specific parameter settings are shown in Table 5.

Table 5 Network parameter settings

Algorithm	Parameter setting
HSVM	H=2, C=100, α = 1.0e − 5
CSA-HSVM	Fl=2.5, AP=0.1, iter=100, NP=20, C=100, α = 1.0e − 5
KNN	K=4
LVQ	η = 0.01, max_epoch=300, Num_Compet=20
SAE-HSVM	Number_AE=2, H=2, C=100, α = 1.0e − 5
SAE-LVQ	Number_AE=2, η = 0.01, max_epoch=300, Num_Compet=20

The 12-dimensional situational air combat information parameter $\boldsymbol{X} = [x_u, y_u, z_u, v_u, \gamma_u, \psi_u, x_t, y_t, z_t, v_t, \gamma_t, \psi_t]$ is used as the training input, 15 types of confrontation samples are generated by the UCAV model, and the number of samples reaches 3 310 groups. The C-LSHADE-Means is used to assign data labels, and a confrontation process with 365 sets of data is selected as the test set. Each algorithm is run 20 times, the accuracy and time are counted. The accuracy rate, root-mean-square error (RMSE), mean absolute percentage error (MAPE), and kappa coefficient are used as the performance index for situation assessment. The experimental simulation environment is Windows 10, the CPU is 2.80 GHz, 16G memory, and the running software is Matlab2019b.

Fig. 16(a) shows the test set assessment result. Fig. 16(b) shows the test set assessment error. It can be seen that the SAE-LVQ method has the better effect. On the test set, only three sets of data situation assessment are wrong.

Table 6 summarizes the results of SAE-LVQ and the comparison algorithm. Through the assessment results of SAE-LVQ and LVQ, and SAE-HSVM and HSVM, it can be seen that using SAE to reconstruct the air combat information as input can significantly improve the accuracy, RMSE, MAPE and kappa coefficients. At the same time, compared with other comparison methods, SAE-LVQ is the best in accuracy indexes, and SAE-LVQ is relatively poor in time consumption, but the average single step time of 1.024e−04 s can also meet the timeliness performance requirements.

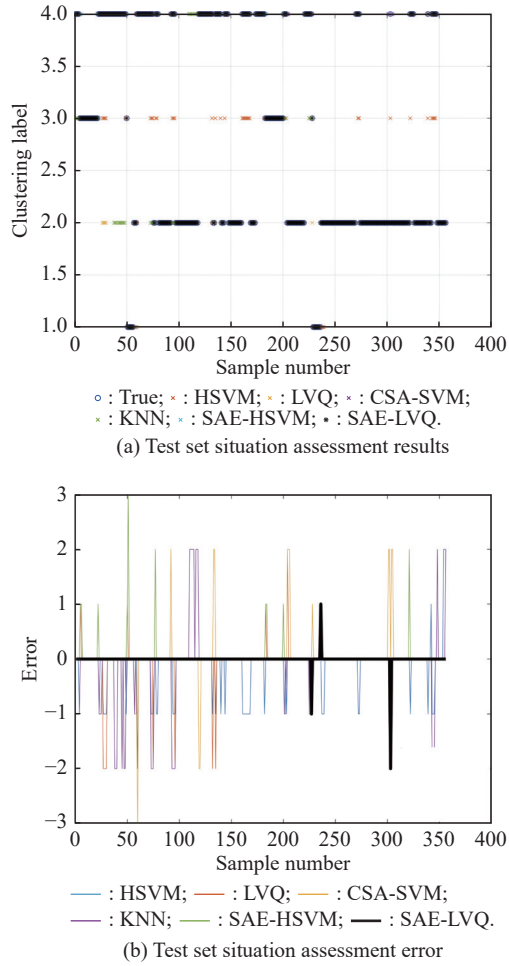

Fig. 16 Test set assessment results and errors

Table 6 Comparison of performance indexes

Classifier	Mean (SD)				
	Accuracy/%	RMSE	MAPE/%	Kappa	Time
HSVM	86.704(4.29e−01)	0.120 8(1.12e−02)	4.026 2(4.61e−01)	0.791 2(6.4e−03)	9.183e−05(1.862e−05)
LVQ	94.663(2.81e−01)	0.046 8(4.3e−03)	2.660 7(1.95e−01)	0.911 3(4.7e−03)	3.412e−05(3.247e−06)
CSA-SVM	94.10(7.43e−01)	0.062(9.7e−03)	4.681(4.56e−01)	0.904(1.20e−02)	3.16e−04(7.34e−04)
KNN	88.015(6.13e−01)	0.055(1.27e−02)	6.99(7.43e−01)	0.804(1.74e−02)	7.674e−05(5.152e−05)
SAe−HSVM	96.910(2.81e−01)	0.035 6(5.8e−03)	2.122 3(5.49e−01)	0.948 6(4.6e−03)	4.435e−04(6.882e−07)
SAe−LVQ	99.251(1.62e−01)	0.003 7(1.6e−03)	0.538 4(1.46e−01)	0.987 6(2.7e−3)	1.024e−04(1.292e−05)

6. Air combat confrontation analysis

To verify the effectiveness of the assessment model proposed in this paper in practical application, three different confrontation processes are selected from the ACMI system. SAE-LVQ assesses the UCAV and enemy aircraft, according to the results, it can be divided into four global situations, as shown in Table 7. In Table 7, 1 is absolute advantage; 2 is advantage; 3 is disadvantage; 4 is absolute disadvantage.

Table 7 Global situation

Situation	State1	State2	State3	State4	State5	State6	State7	State8
UCAV	1	1	2	2	3	3	4	4
Enemy	1	4	2	3	2	3	1	4
Global situation	Mutual threaten	Advantage	Mutual threaten	Advantage	Disadvantage	Mutual safe	Disadvantage	Mutual safe

6.1 Case 1

A period of head-on confrontation between two aircraft is selected. Among them, UCAV stands for confrontation drone, and enemy refers to the aircraft operated by pilots. Fig. 17(b) and Fig. 17(c) assess the UCAV and enemy aircraft situation, and Fig. 17(d) depicts the global situation. The initial state of UCAV and the enemy aircraft is head-on flight. At this time, the angles of both sides are in a good state, but the distance is too far. Therefore, SAE-LVQ evaluates UCAV in the advantage state in the first 32 samples in Fig. 17(b), and the enemy is also in the advantage state in the first 32 samples in Fig. 17(c). As the distance between the two parties is getting closer, the UCAV and the enemy both make a right-turn maneuver. At this time, the angle and distance of both sides are in good condition, in Fig. 17(b) and Fig. 17(c), SAE-LVQ evaluates that UCAV and enemy are in absolute advantage. According to Table 7, the global situation assessment is carried out, as shown in Fig. 17(d), which is in a mutual threaten situation.

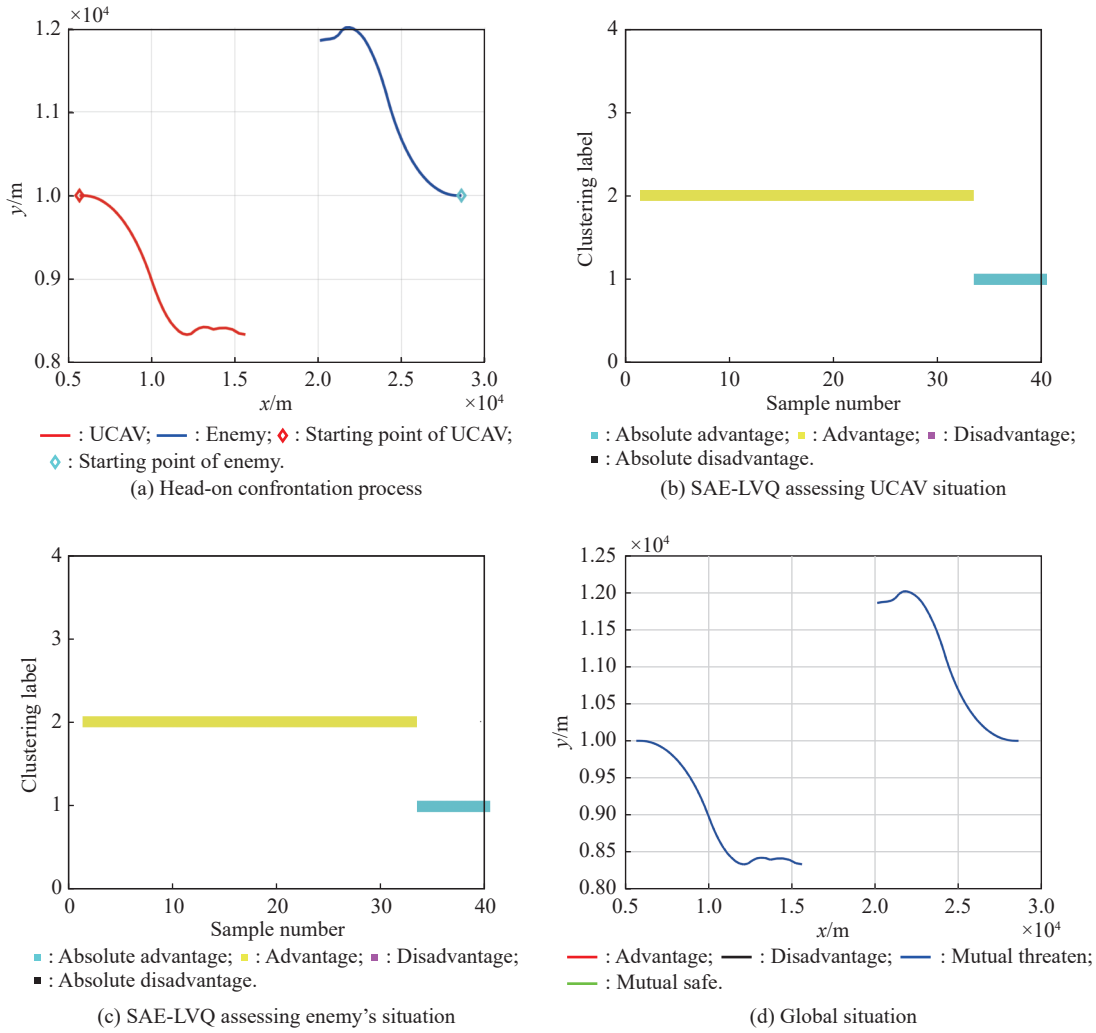

(a) Head-on confrontation process

(b) SAE-LVQ assessing UCAV situation

(c) SAE-LVQ assessing enemy's situation

(d) Global situation

Fig. 17 Situation analysis of Case 1

6.2 Case 2

A tail chase confrontation process is selected. The specific confrontation process is shown in Fig. 18(a). Fig. 18(b) and Fig. 18(c) evaluate the UCAV and enemy aircraft situation, and Fig. 18(d) depicts the global situation. In the initial state, UCAV chases the enemy behind the tail, UCAV is in an advantaged state, as shown in Fig. 18 (b), and the enemy is in a disadvantaged state in Fig. 18 (c). At this time, the global situation is an advantage, which is in line with the actual situation. After that, the enemy makes a right-turn and dive maneuver to try to get rid of the disadvantage. In Fig. 18(c), the enemy turns from a disadvantage to an advantage. In Fig. 18(d), it can be seen that it is in the mutual threat situation. UCAV bites the enemy's tail, but the speed is too fast to cause a forward rush. It is evaluated as a disadvantage in Fig. 18(b), and enemy is also evaluated as a disadvantage in Fig. 18(c). At this time, the global situation is mutual safety. Then the enemy performs a left-turn maneuver. At this time, UCAV is the disadvantage, the enemy is the advantage, and the global situation is the disadvantage. UCAV quickly performs a right turn. The enemy is at a disadvantage, and the global situation is mutually safe. In the end, UCAV adjusts its angle and quickly turns into an advantage, and the enemy is disadvantaged, so the global situation is an advantage, and the confrontation ends.

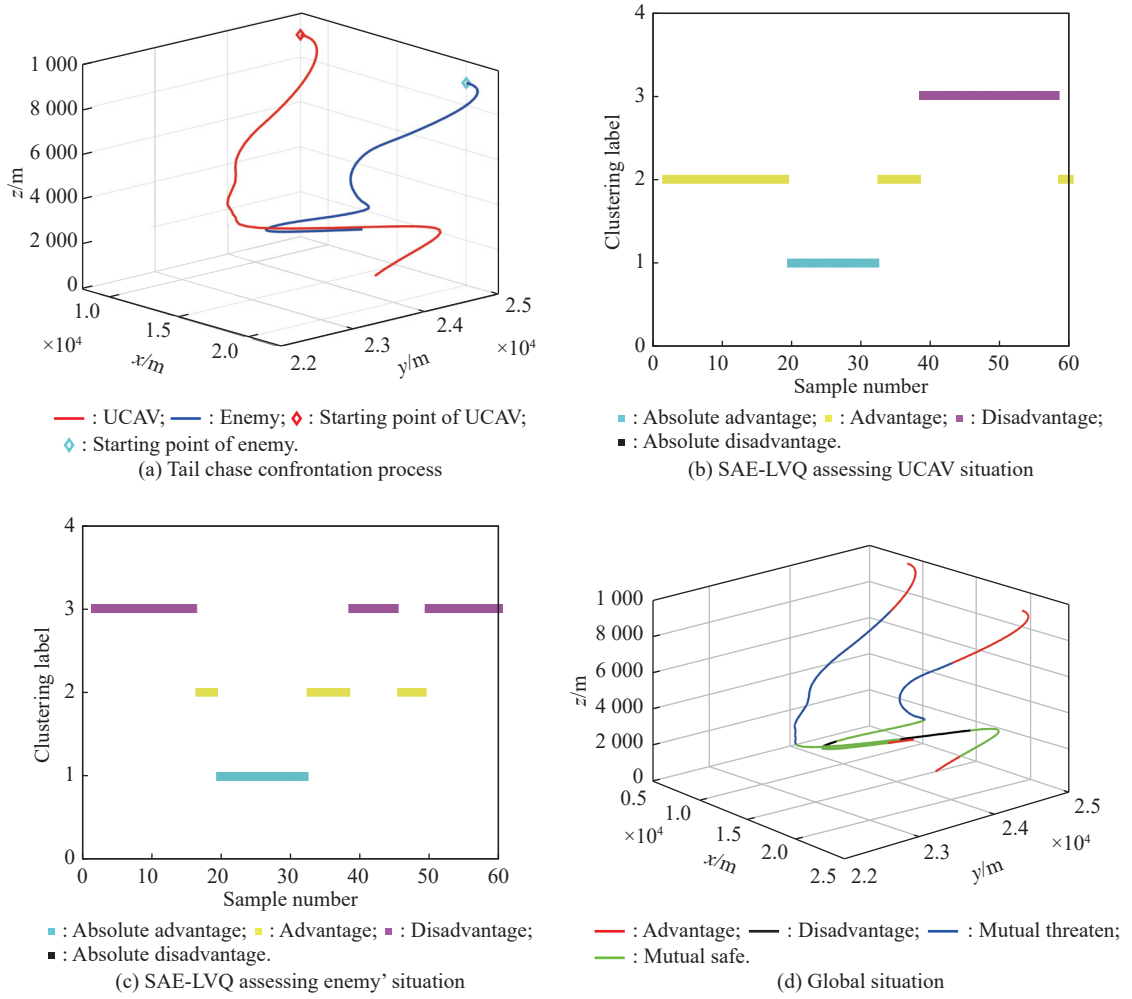

Fig. 18 Situation analysis of Case 2

6.3 Case 3

A relatively complicated process of close combat confrontation is shown in Fig. 19(a). Fig. 19(b) and Fig. 19(c) evaluate the UCAV and enemy aircraft situation, and Fig. 19(d) depicts the global situation. In the initial stage, the two sides approached head-on, with a good angle but a long distance, it is a mutual threat situation. With the continually decreasing of distance, UCAV and the enemy are both in the advantaged state, since then, the two sides continuously make large overload maneuvers, and constantly adjust the angle. In Fig. 19(b) and Fig. 19 (c), it can be seen that the situation of UCAV and enemy is constantly alternating between absolute advantage and abso-

lute disadvantage. The global situation also alternates from the mutual threat, mutual safe and advantage. In the end, the two parties leave in the opposite direction, and the global situation is the mutual safe.

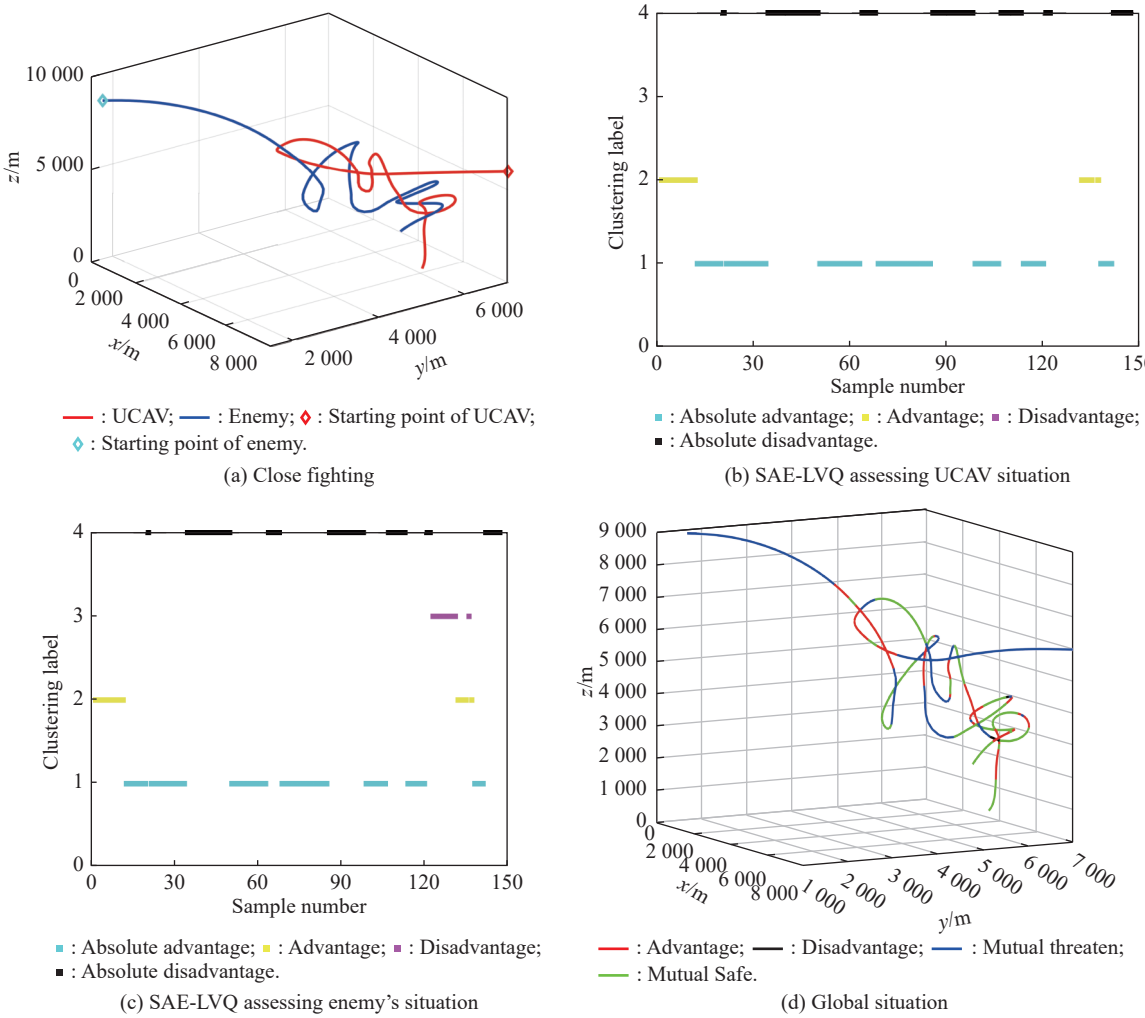

Fig. 19 Situation analysis of Case 3

7. Conclusion and future work

In the air combat situation assessment, a data-driven assessment method is proposed. First, the C-LSHADE-Means clustering method is used to mine air combat situation knowledge, and then the SAE-LVQ model is constructed for situation assessment. The following conclusions are obtained through simulation experiments:

(i) The C-LSHADE-Means method and seven clustering algorithms are compared in the UCI data set. Through four clustering indexes, it has been proved to have better clustering performance. It can extract air combat situation knowledge by using confrontation data, and overcome the shortcomings of traditional methods such as excessive subjectivity and prior knowledge dependence.

(ii) The situational assessment model based on LVQ-SAE performs better than HSVM, RBF, DNN, LVQ and SAE-HSVM in terms of assessment accuracy, it can also meet the high timeliness requirements of air combat assessment.

(iii) Using ACMI data for assessment, the results show that the method proposed in this paper is in line with the actual situation and can better reflect the global situation of air combat.

The future research direction is to combine situation assessment with maneuver decision-making, and use situation assessment results to guide maneuver decision-making.

References

[1] LUNSFORD I, BRADLEY T H. Evaluation of unmanned aerial vehicle tactics through the metrics of survivability.

Journal of Defense Modeling and Simulation-Applications Methodology Technology, 2021, 19(4): 855–864.
[2] DONG Y Q, AI J L, LIU J Q. Guidance and control for own aircraft in the autonomous air combat: a historical review and future prospects. Journal of Aerospace Engineering, 2019, 133(16): 5943–5991.
[3] YANG K B, DONG W H, CAI M, et al. UCAV air combat maneuver decisions based on a proximal policy optimization algorithm with situation reward shaping. Electronics, 2022, 11(16): 2602.
[4] FU L, CHANG F H, XU J, et al. Research of air combat situation assessment method. Proc. of the International Conference on Digital Manufacturing & Automation, 2012. DOI: 10.1109/ICDMA.2012.155.
[5] ZHAO K X, HUANG C Q. Air combat situation assessment for UAV based on improved decision tree. Proc. of the 30th Chinese Control and Decision Conference, 2018. DOI: 10.1109/CCDC.2018.8407414.
[6] ZHANG H P, HUANG C Q. Maneuver decision-making of deep learning for UCAV thorough azimuth angles. IEEE Access, 2020, 8: 12976–12987.
[7] ZHANG C K, CHENG Y, HE Z Q, et al. Method of dynamic air combat threat evaluation based on time series. Proc. of the 35th Chinese Control Conference, 2016. DOI:10.1109/ChiCC.2016.7554892.
[8] YING Z, TANG Y C, ZHAO X Z. Novel uncertainty management approach for air combat situation assessment based on improved belief entropy. Entropy, 2019, 21(5): 495–506.
[9] XU X M, YANG R N, FU Y. Situation assessment for air combat based on novel semi-supervised naive Bayes. Journal of Systems Engineering and Electronics, 2018, 29(4): 768−779.
[10] LU C G, ZHOU Z L, LIU H Q, et al. Situation assessment of far-distance attack air combat based on mixed dynamic bayesian networks. Proc. of the 37th Chinese Control Conference, 2018. DOI: 10.23919/ChiCC.2018.8483074.
[11] HE X M, ZU W, CHANG H X, et al. Autonomous maneuvering decision research of UAV based on experience knowledge representation. Proc. of the Chinese Control and Decision Conference, 2016. DOI: 10.1109/CCDC.2016.7530973.
[12] XUAN Y B, HUANG C Q, LI W X. Air combat situation assessment by gray fuzzy Bayesian network. Applied Mechanics and Materials, 2011, 69: 114–119.
[13] SUN Z L, YANG H W, HU W D, et al. Situation assessment for air combat based on the Bayesian networks technology. Proceedings of SPIE - The International Society for Optical Engineering, 2006. DOI: 10.1117/12.657673.
[14] NARAYANA R P, SUDESH K K, GIRIJA G, et al. Situation and threat assessment in BVR combat. Proc. of the AIAA Guidance, Navigation & Control Conference, 2011. DOI: 10.2514/6.2011-6241.
[15] MA S D, YANG G Q, ZHANG H Z, et al. Target threat level assessment technology based on cloud model and Bayesian revision in air combat simulation. Proc. of the 35th Chinese Control Conference, 2016. DOI: 10.1109/ChiCC.2016.7554903.
[16] VIRTANEN K, RAIVIO T. Modeling pilot's sequential maneuvering decisions by a multistage influence diagram. Journal of Guidance, Control, and Dynamics, 2004, 27(4): 665–677.
[17] KAI V, JANE K, TUOMAS R. Modeling air combat by a moving horizon influence diagram game. Journal of Guidance, Control, and Dynamics, 2006, 29(5): 1080–1091.
[18] ALAM S, DOBBIE G, KOH Y S, et al. Research on particle swarm optimization-based clustering: a systematic review of literature and techniques. Swarm and Evolutionary Computation, 2014, 17: 1–13.
[19] NANDA S J, PANDA G. A survey on nature inspired metaheuristic algorithms for partitional clustering. Swarm and Evolutionary Computation, 2014, 16: 1−18.
[20] JOSE G A, GOMEZ F W. Automatic clustering using nature-inspired metaheuristics: a survey. Applied Soft Computing, 2016, 41: 192–213.
[21] HRUSCHK E R, CAMPELLO R J G B, FREITAS A A, et al. A survey of evolutionary algorithms for clustering. IEEE Trans. on Systems, Man, and Cybernetics: Part C (Applications and Reviews), 2009, 39(2): 133–155.
[22] INKAYA T, KAYALGIL S, ZDEMIREL N E. Ant colony optimization-based clustering methodology. Applied Soft Computing, 2015, 28: 301–311.
[23] REFAAT M M, ALEEM S H E A, ATIA Y, et al. Multi-stage dynamic transmission network expansion planning using LSHADE-SPACMA. Applied Sciences, 2021, 11(5): 2155.
[24] MOHAMED A W, HADI A A, FATTOUH A M, et al. LSHADE with semi-parameter adaptation hybrid with CMA-ES for solving CEC 2017 benchmark problems. Proc. of the IEEE Congress on Evolutionary Computation, 2017. DOI: 10.1109/CEC.2017.7969307.
[25] ZHANG J Q, SANDERSON A C. JADE: adaptive differential evolution with optional external archive. IEEE Trans. on Evolutionary Computation, 2009, 13(5): 945–958.
[26] ELLIACKIN F, MARIANA M, HUGO V S, et al. Swarm intelligence for clustering —a systematic review with new perspectives on data mining. Engineering Applications of Artificial Intelligence, 2019, 82: 313−329.
[27] BRUSCO M J, STEINLEY D. A comparison of heuristic procedures for minimum within-cluster sums of squares partitioning. Psychometrika, 2007, 72(4): 583–600.
[28] WANG Y, LI H X, HUANG T W, et al. Differential evolution based on covariance matrix learning and bimodal distribution parameter setting. Applied Soft Computing Journal, 2014, 18(1): 232–247.
[29] STORN R. Differential evolution —a simple and efficient heuristic for global optimization over continuous space. Journal of Global Optimization, 1997, 11: 341–359.
[30] XUE J K, SHEN B. A novel swarm intelligence optimization approach: sparrow search algorithm. Systems Science & Control Engineering, 2020, 8(1): 22–34.
[31] LI X G, ZHU J, SHI H R, et al. Surface defect detection of seals based on k-means clustering slgorithm and particle swarm optimization. Scientific Programming, 2021, 2021: 3965247.
[32] HEIDARI A A, SEYEDALI M, HOSSAM F, et al. Harris hawks optimization: algorithm and applications. Future Generation Computer Systems, 2019, 97(12): 849–872.
[33] KOHLI M, ARORA S. Chaotic grey wolf optimization algorithm for constrained optimization problems. Journal of Computational Design and Engineering, 2018, 5(4): 458–472.
[34] ESMAT R, HOSSEIN N, SAEID S. GSA: a gravitational search algorithm. Information Sciences, 2009, 179(13): 2232–2248.
[35] HANCER E, KARABOGA D. A comprehensive survey of traditional, merge-split and evolutionary approaches proposed for determination of cluster number. Swarm and Evo-

lutionary Computation, 2017, 32: 49−67.
[36] GAO J, ZHAO L, CHEN Z K, et al. ICFS: an improved fast search and find of density peaks clustering algorithm. Proc. of the 14th International Conference on Dependable, Autonomic and Secure Computing, 2016. DOI: 10.1109/DASC-PICom-DataCom-CyberSciTec.2016.103.
[37] WANG Z Q, YU Z W, CHEN C L P, et al. Clustering by local gravitation. IEEE Trans. on Cybernetics, 2017, 48(5): 1383–1396.
[38] REZAEE M J, ESHKEVARI M, SABERI M, et al. GBK-means clustering algorithm: an improvement to the K-means algorithm based on the bargaining game. Knowledge-Based Systems, 2021, 213: 106672.
[39] ZHANG Z R. Research on key technologies of autonomous close-range air combat for unmanned combat aircraft. Xi'an: Air Force Engineering University, 2019. (in Chinese)
[40] TAN S X. An intrusion detection method based on stacked autoencoder and support vector machine. Journal of Physics: Conference Series, 2020, 1453(1): 012010–012016.
[41] ZABALZA J, REN J C, ZHENG J B, et al. Novel segmented stacked autoencoder for effective dimensionality reduction and feature extraction in hyperspectral imaging. Neurocomputing, 2016, 185: 1–10.
[42] LU X T, WANG H, DONG W S, et al. Learning a deep vector quantization network for image compression. IEEE Access, 2019, 7: 118815–118825.
[43] KAYAMA M, SUGITA Y, MOROOKA Y. Sensor diagnosis system combining immune network and learning vector quantization. Electrical Engineering in Japan, 1996, 117(5): 44–56.
[44] LIU J Y, LIANG Y C, SUN X Y. Application of learning vector quantization network in fault diagnosis of power transformer. Proc. of the International Conference on Mechatronics & Automation, 2009. DOI: 10.1109/ICMA.2009.5246676.
[45] TANG F Z, TINO P, YU H B. Generalized learning vector quantization with log-Euclidean metric learning on symmetric positive-definite manifold. IEEE Trans. on Cybernetics, 2022. DOI: 10.1109/TCYB.2022.3178412.
[46] ZHANG X Y, QIU D Y, CHEN F. Support vector machine with parameter optimization by a novel hybrid method and its application to fault diagnosis. Neurocomputing, 2015, 149: 641–651.
[47] WANG L T, ZHANG J X, ZHANG J H, et al. Application of crow search algorithm in SVM parameter optimization. Computer Engineering and Applications, 2019, 55(21): 213–218. (in Chinese)
[48] MAITY A, PRAKASAM P, BHARGAVA S. Machine learning based KNN classifier: towards robust, efficient DTMF tone detection for a noisy environment. Multimedia Tools and Applications, 2021, 80(19): 29765–29784.

Biographies

XIE Lei was born in 1997. He received his bachelor degree in arms engineering and master degree in armament science and technology from Air Force Engineering University, Xi'an, China. He is currently pursuing his doctor degree in Air Force Engineering University, Xi 'an, Shaanxi, China. His research interests include air combat, intelligent optimization algorithm, maneuvering decision, and situation assessment.
E-mail: 310370487@qq.com

TANG Shangqin was born in 1984. He received his bachelor and Ph.D. degrees in arms engineering from Air Force Engineering University in 2007 and 2013, respectively. His research interests include air combat maneuver decision, intention recognition, and situation assessment.
E-mail: 630909448@qq.com

WEI Zhenglei was born in 1991. He received his B.S., M.S., and Ph.D. degrees in armament science and technology from Air Force Engineering University. He is an engineer in China Aerodynamics Research & Development Center. His research interests include maneuvering prediction and maneuvering decision.
E-mail: zhenglei_wei@126.com

XUAN Yongbo was born in 1984. He received his Ph.D. degree from Air Force Engineering University in 2012. He is an engineer in Beijing Blue Sky Innovation Center for Frontier Science. His research interest is general technology.
E-mail: 398791736@qq.com

WANG Xiaofei was born in 1990. He received his Ph.D. degree of weapon science and technology from Air Force Engineering University in 2020. He is an engineer in Beijing Blue Sky Innovation Center for Frontier Science. His research interests are evolutionary algorithms and UCAV air combat decision.
E-mail: wxf825421673@163.com